

# Pseudo-single photon state and its application to secure quantum communication

Seung-Woo Lee<sup>1</sup> and Jaewan Kim<sup>2</sup>

<sup>1</sup>Quantum Universe Center, Korea Institute for Advanced Study, Seoul 02455, Korea

<sup>2</sup>School of Computational Sciences, Korea Institute for Advanced Study, Seoul 02455, Korea

We introduce an optical quantum state that can fundamentally mimic a single photon state not only with respect to the number of photons but also in terms of an indeterminate phase. It becomes close to a perfect single photon state with almost unit fidelity as well as exhibits fundamental features of single photons such as antibunching and Hong-Ou-Mandel interference. The emergence and vanishing of single photon characteristics can be directly observed by changing two variables, i.e., mean photon number and number of phases. Moreover, we propose a feasible scheme to generate such a state at room temperature by using atomic vapor in hollow-core optical fiber, which is suitable for integration in fiber-optic quantum network. Finally, we demonstrate that quantum key distribution (QKD) with these states outperforms the typical approach using weak coherent states.

Single photons are ideal carriers of quantum information and primary resources to explore quantum mechanics. Quantum principles such as complementarity and the impossibility of cloning quantum state [1] constitute the fundamental basis of the security of quantum communications [2–6]. Especially, the uncertainty in the measurement of two conjugate variables on single photons is the key feature of quantum key distribution (QKD) protocols [2, 4, 5]. Moreover, their characteristics such as antibunching and Hong-Ou-Mandel interference [7] play a major role in implementing quantum communications [8–10]. An ideal single photon source is, however, challenging [11] despite recent substantial progress [12, 13].

A natural question that comes to mind may be whether single photons can be attained by strongly attenuating conventional lasers, for example, by dividing the pulse infinite many times via beam splitters. An attenuated laser, however, contains more than single photons with a nonzero probability following a Poisson distribution. It can be described by a weak coherent state (WCS) in the form of  $|\sqrt{\mu}e^{i\theta}\rangle = e^{-\mu/2} \sum_{n=0}^{\infty} (\sqrt{\mu}e^{i\theta})^n / \sqrt{n!} |n\rangle$ , where  $\mu$  is the mean photon number,  $\theta$  is the phase, and  $|n\rangle$  is the photon number state. It indeed distributes the uncertainty (roughly) equally between phase and amplitude so that the phase is not indeterminate. Moreover, it never exhibits the behaviors of single photons, i.e., antibunching and Hong-Ou-Mandel interference. Although, in certain applications (e.g. QKD), the multi-photon issue of WCS can be circumvented by the decoy state method [14–16] for practical use, it requires a perfectly randomized phase  $\theta$  [17]. Recent attempts to yield single photon behaviors and multi-photon interference from phase randomized WCS [18–21] are in fact indirect observations through data reconstruction (but not the genuine exhibitions) of such behaviors. Therefore, it is still obscure what constitutes the fundamental characteristics of single photons and how single photon nature can emerge from optical states including multiple photons by attenuation.

We here introduce an optical quantum state that can fundamentally mimic single photons with respect to both the mean photon number and indeterminate phases. This

state, hereafter referred to as *pseudo-single photon state* (PSP), can be defined as a superposition of WCSs equally distributed on a circle in phase space with a discretized phase  $2\pi/d$ . Remarkably, not only it becomes close to the ideal single photon state with almost unit fidelity but also it exhibits the fundamental features of single photons such as antibunching and Hong-Ou-Mandel interference. Its single photon characteristics are tunable with two parameters  $\mu$  and  $d$ ; As either  $\mu$  decreases or  $d$  increases, PSPs and their behaviors become closer to ideal single photons. It reveals the fact that the uncertainty between photon number and phase indeed constitutes the characteristics of single photons. In addition, we propose a scheme to generate PSPs with fast response time at room temperature employing atomic vapor in hollow-core photonic crystal fibers [22, 23], which is feasible within current optical technologies and suitable for the application to fiber optic communication. Finally, by applying PSPs for the implementation of QKD, we demonstrate higher key generation rates over longer distances than the typical approach using phase randomized WCSs, which is a representative example revealing the quantum advantage of the uncertainty principle over statistical randomization. We expect that our work opens an alternative route for exploring fundamental features of single photons and to the realization of secure quantum communications.

*Pseudo-single photon states-* We start with the definition of pseudo-number states. In contrast to ideal photon number states having continuous random phase, we here consider discretized phases  $2\pi/d$  with an integer  $d$ , corresponding to equally distributed coherent states on a circle in phase space, e.g.  $\{|\sqrt{\mu}\rangle, |\sqrt{\mu}\omega\rangle, \dots, |\sqrt{\mu}\omega^{d-1}\rangle\}$  with  $\omega = \exp(2\pi i/d)$ . We define pseudo-number states as the maximally superposed states of the coherent states

$$|j_d\rangle = \frac{1}{\sqrt{\mathcal{N}_{\mu,j}}} \sum_{q=0}^{d-1} \omega^{-jq} |\sqrt{\mu}\omega^{q+\delta}\rangle \quad (1)$$

where  $j \in \{0, 1, \dots, d-1\}$ ,  $\mathcal{N}_{\mu,j}$  is the normalization factor dependent on  $\mu$  and  $j$ , and  $\delta$  is the reference phase (we set hereafter  $\delta = 0$  unless necessary). It can be also rewritten

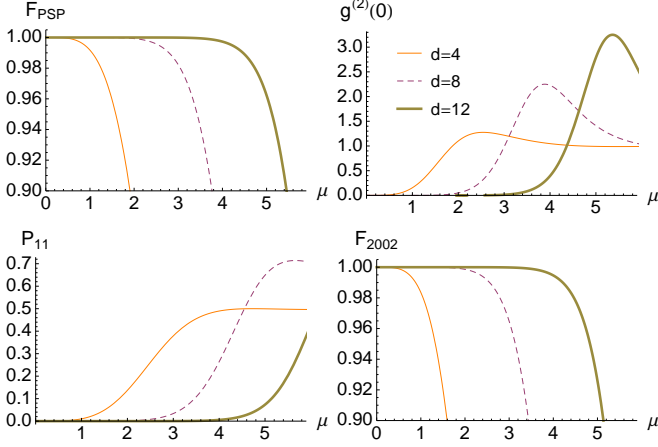


FIG. 1.  $F_{\text{PSP}}$ : the fidelities between ideal single photon state and PSPs,  $g^{(2)}(0)$ : the 2nd-order correlation function of PSPs,  $P_{11}$ : the probabilities for detecting photons at both output modes of beam splitter which two PSPs enter different input modes,  $F_{2002}$ : the fidelities between the state in output modes of the beam splitter and  $(|2\rangle|0\rangle - |0\rangle|2\rangle)/\sqrt{2}$ , by changing the mean photon number  $\mu$  for  $d = 4, 8, 12$ .

by  $|j_d\rangle = (d/\sqrt{\mathcal{N}_{\mu,j}})e^{-\mu/2} \sum_{n \in \mathbb{S}_j} \mu^{n/2}/\sqrt{n!}|n\rangle$ , where  $\mathbb{S}_j = \{n|j \equiv n \pmod{d}\}$  [24, 25]. The coherent state on a circle is written conversely with the pseudo-number states as  $|\sqrt{\mu}\omega^q\rangle = (1/\sqrt{d}) \sum_{j=0}^{d-1} \omega^{qj} \sqrt{\mathcal{N}_{\mu,j}/d}|j_d\rangle$ . We note that  $|j_d\rangle$  and  $|\sqrt{\mu}\omega^q\rangle$  represent conjugate variables connected by the number-phase uncertainty.

When  $\mu$  is small,  $|j_d\rangle$  can mimic ideal number states, while for large  $\mu$  (i.e.  $\sqrt{\mu} > d$ ) it nearly constitutes  $d$ -dimensional orthonormal basis [25]. We can observe that  $|j_d\rangle$  becomes closer to  $|j\rangle$  as  $\mu$  gets smaller or  $d$  increases with the fidelity  $F(|j\rangle, |j_d\rangle) = |\langle j|j_d\rangle|^2 = (d^2/\mathcal{N}_{\mu,j})e^{-\mu} \mu^j/j!$ . For example,  $F_{\text{PSP}} \equiv F(|1\rangle, |1_d\rangle)$  approaches to unit as  $\mu$  decreases or  $d$  increases as shown in Fig. 1. We can also analytically see that, either in the limit  $d \rightarrow \infty$  with finite  $\mu$  or in the limit  $\mu \rightarrow 0$  with finite  $d$ ,  $F(|1\rangle, |1_d\rangle) \rightarrow 1$  (details in Appendix). We thus hereafter call  $|1_d\rangle$  with arbitrarily small  $\mu$  as pseudo-single photon state (PSP). The PSP becomes an odd cat state [26] when  $d = 2$ , well known to get closer to  $|1\rangle$  as  $\mu \rightarrow 0$ , while PSPs with higher  $d$  approach  $|1\rangle$  in the wider range of  $\mu$ . We can also analyze the effects of photon losses on PSPs (details in Appendix). Under losses (with a transmission rate  $\eta$ ) [27], the state of PSP with mean photon number  $\mu$  is changed into a mixed state  $\rho_d = \{1 - \mu(1 - \eta)\}|1'_d\rangle\langle 1'_d| + \mu(1 - \eta)|0'_d\rangle\langle 0'_d|$ , where  $|1'_d\rangle$  and  $|0'_d\rangle$  are the pseudo-single and -vacuum states with mean photon number  $\mu' = \mu\eta$ .

*Single photon features-* We investigate the single photon characteristics of PSPs by changing  $d$  and  $\mu$ :

i) Antibunching: It refers to sub-Poissonian statistics of photons [28], characterized with the 2nd-order correlations function  $g^{(2)}(0) = \langle a^\dagger a^\dagger a a \rangle / \langle a^\dagger a \rangle^2 < 1$ , while

coherent states are in Poissonian statistics  $g^{(2)}(0) = 1$ . For PSP with arbitrary  $\mu$  and  $d$ ,  $g^{(2)}(0)$  can be calculated (see Appendix) and plotted as in Fig.1. The sub-Poissonian statistics with nearly  $g^{(2)}(0) = 0$  are observed in small  $\mu$  region that becomes wider as  $d$  increases. Note that, as  $\mu$  increases, first a transition occurs from sub-to super-Poissonian, and then the statistics gradually become Poissonian  $g^{(2)}(0) = 1$ .

ii) Two-photon (Hong-Ou-Mandel) interference: Assume that two PSPs with given  $\mu$  and  $d$  enter different input modes of a beam splitter. The probability for detecting photons at both output modes,  $P_{11}$ , can be then calculated (see Appendix) and plotted as in Fig. 1. The fidelity between the state in output modes and  $(|2\rangle|0\rangle - |0\rangle|2\rangle)/\sqrt{2}$ , referred to as  $F_{2002}$ , is also presented in Fig. 1. They show that two-photon interference occurs and becomes more evident as increasing  $d$  or decreasing  $\mu$ . This is stark contrast to phase randomized WCSs that cannot exhibit such an interference even with  $\mu \rightarrow 0$ . For odd cat states (PSP with  $d = 2$ ), despite  $P_{11} = 0$  for any  $\mu$ ,  $F_{2002}$  is close to 1 only with  $\mu \rightarrow 0$  (see Appendix), while PSPs with higher  $d$  (for example, with  $d = 8$ ) show clear two-photon interference with a wider range of  $\mu$  ( $\mu \lesssim 2$ ) as shown in Fig. 1.

In general, two different PSPs (e.g either with different  $\mu$ ,  $d$ , or  $\delta$ ) can exhibit two-photon interference that becomes clearer as the overall mean photon number decreases or the overall number of phases increases (details in Appendix). Note that the maximum interference occurs between the same PSPs when the overall number of photons and phases are fixed. This manifests the fact that they are the most indistinguishable from each other.

*Generation scheme-* We present a scheme to generate PSPs with a feasible technique. Atomic vapor in hollow-core photonic crystal fiber (HC-PCF) is a promising platform to realize photon-level interactions at room temperature [22, 23, 29–33] such as all-optical switches [29, 30] and quantum memories [32]. Particularly, cross

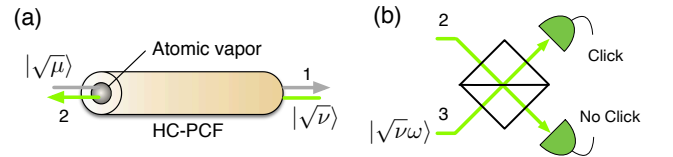


FIG. 2. (a) A generation scheme of the pseudo-number states with atomic vapor confined in hollow-core photonic crystal fiber (HC-PCF). A WCS  $|\sqrt{\mu}\omega\rangle$  enters mode 1, while a strong coherent states  $|\sqrt{\mu'}\omega\rangle$  enters mode 2. Exemplary details are in Ref. [22, 23] (b) A measurement for the discrimination of PSP from other pseudo-number states. The detection event that only the upper detector clicks (while the lower does not) guarantees the generation of PSP in the output mode 1, which is referred to as a triggered event (otherwise as non-triggered events) in our scheme.

phase modulation has been recently realized with rubidium (Rb) atoms filled in HC-PCF in Ref. [22, 23]. Cross-phase shift can be effectively manipulated with fast response time and low transmission loss and without self-Kerr effect [22, 23]. Moreover, it is suitable for the integration with fiber optic communication network (details in Appendix).

For generating PSPs, suppose that lasers in coherent states  $|\sqrt{\mu}\rangle_1|\sqrt{\nu}\rangle_2$  go through the two modes (1 for signal 2 for meter) of atomic vapor filled HC-PCF as illustrated in Fig. 2(a). The interaction Hamiltonian can be written by  $-\hbar\chi^{(3)}\hat{n}_1\hat{n}_2$  for time  $t$  with the number operator  $\hat{n}_i$  in  $i$ th mode. We assume that  $\mu$  is small, while  $\nu$  is large enough such that  $\sqrt{\nu} \gtrsim 2\pi/\chi^{(3)}t$ . Without loss of the generality, we set  $d \equiv 2\pi/\chi^{(3)}t$  as an integer  $\geq 2$ , which is a tunable parameter by changing e.g. the atomic density or length of vapor filled HC-PCF. The state in output modes is then written by (details in Appendix)

$$e^{\frac{2\pi i}{d}\hat{n}_1\hat{n}_2}|\sqrt{\mu}\rangle_1|\sqrt{\nu}\rangle_2 \rightarrow \sum_{j=0}^{d-1} \frac{\sqrt{\mathcal{N}_{\mu,j}}}{d} |j_d\rangle_1 |\sqrt{\nu}\omega^j\rangle_2. \quad (2)$$

A phase detection in mode 2 (i.e. discrimination of  $j \in \{0, 1, \dots, d-1\}$ ) can identify  $|j_d\rangle$  generated in mode 1. The probability of the generation of each  $|j_d\rangle$  is given by

$$P_{\mu,j} = \frac{\mathcal{N}_{\mu,j}}{d^2} = e^{-\mu} \sum_{n \in \mathbb{S}_j} \frac{\mu^n}{n!}. \quad (3)$$

With the choice of  $\sqrt{\nu} > d$ , as the overlap between the coherent states  $|\sqrt{\nu}\omega^j\rangle$  with different  $j$  on a circle is negligible, one can consider heterodyne measurements to fully discriminate  $j \in \{0, 1, \dots, d-1\}$ . An alternative and more realistic scheme to distinguish  $|1_d\rangle$  only from others  $|j(\neq 1)_d\rangle$  can be implemented by using inefficient on-off detectors as illustrated in Fig. 2 (b). The detection event that only the upper detector clicks guarantees that the output state in mode 1 is  $|1_d\rangle$ , which we treat as a triggered event (and others as non-triggered events). The probability of the triggered event is

$$\eta_{\nu,j}^{(t)} = \left| \langle 0 | \sqrt{\eta_{\text{det}}\nu}(\omega^j - \omega) / \sqrt{2} \rangle \right|^2 = \exp[-\eta_{\text{det}}\nu|\omega^j - \omega|^2/4], \quad (4)$$

where  $\eta_{\text{det}}$  is the efficiency of the photon detectors. The dark count at the detector is assumed here to be negligible. The probability of the non-triggered event is then  $\eta_{\nu,j}^{(nt)} = 1 - \eta_{\nu,j}^{(t)}$ . Note that  $\eta_{\nu,1}^{(t)} = 1$  and  $\eta_{\nu,1}^{(nt)} = 0$ . On the other hand,  $\eta_{\nu,j \neq 1}^{(t)}$  tends to decrease as  $\nu$  or  $\eta_a$  increases, while it increases as  $d$  increases. Note that a low detection efficiency  $\eta_{\text{det}}$  can be compensated here with the choice of large  $\nu$ .

*Application to secure quantum communications-* PSPs can be directly applied to quantum communications, particularly for fiber-optic based implementations. The single photon behaviors of PSPs enables to implement ele-

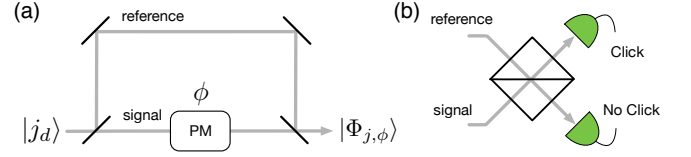


FIG. 3. (a) Schematic of the phase encoding QKD scheme on Alice's side. A prepared pseudo-number state  $|j_d\rangle$  is separated into two (one is for signal and the other is for reference) by a 50:50 beam splitter.  $\phi \in \{0, \pi/2, \pi, 3\pi/4\}$  is encoded into the signal with a phase modulator (PM). (b) X or Y basis measurement on Bob's side.

mentary tasks of quantum communications such as Bell-state measurements. Further, the tunable characteristics of PSPs with two variables,  $\mu$  and  $d$ , enrich their potential use in quantum optical applications.

We here consider a representative example: QKD with PSPs. Suppose that  $|j_d\rangle$  with mean photon number  $2\mu$  is prepared on Alice's side. It enters a phase encoding setup illustrated in Fig. 3(a). The output state is then given by

$$|\Phi_{j,\phi}\rangle = \frac{1}{\sqrt{\mathcal{N}_{2\mu,j}}} \sum_{q=0}^{d-1} \omega^{-jq} |\sqrt{\mu}\omega^q\rangle_r |\sqrt{\mu}\omega^{q+k}\rangle_s, \quad (5)$$

where the subscript  $s(r)$  denotes the signal(reference) state, and  $k = \phi d/2\pi$  denotes the rotated phase in the signal mode for encoding. Note that the randomness of the reference phase is guaranteed by the superposition of the states  $|\sqrt{\mu}\omega^q\rangle$  with  $q \in \{0, \dots, d-1\}$ . This is contrast to the conventional QKD encoding scheme using WCS in the form of  $|\sqrt{\mu}\omega^q\rangle_r |\sqrt{\mu}\omega^{q+k}\rangle_s$ , which requires an additional process for the phase randomization with an active phase modulator and a random number generator [34]. For the Bennett and Brassard 1984 protocol (BB84) [2], logical 0 and 1 are encoded either in X or Y basis, i.e.,  $\{|0_x\rangle_j, |1_x\rangle_j\} = \{|\Phi_{j,0}\rangle, |\Phi_{j,\pi}\rangle\}$  or  $\{|0_y\rangle_j, |1_y\rangle_j\} = \{|\Phi_{j,\pi/2}\rangle, |\Phi_{j,3\pi/4}\rangle\}$ . On Bob's side, a measurement is performed either in X or Y basis as illustrated in Fig. 3(b). For X-basis measurement, the reference and signal states enter the input modes of a beam splitter such that

$$\begin{aligned} |0_x\rangle_j &= \frac{1}{\sqrt{\mathcal{N}_{2\mu,j}}} \sum_{q=0}^{d-1} \omega^{-jq} |\sqrt{\mu}\omega^q\rangle_r |\sqrt{\mu}\omega^q\rangle_s \rightarrow |j_d\rangle|0\rangle \\ |1_x\rangle_j &= \frac{1}{\sqrt{\mathcal{N}_{2\mu,j}}} \sum_{q=0}^{d-1} \omega^{-jq} |\sqrt{\mu}\omega^q\rangle_r |-\sqrt{\mu}\omega^q\rangle_s \rightarrow |0\rangle|j_d\rangle. \end{aligned}$$

Thus, two logical encoding (either 0 and 1) can be discriminated by performing photon on-off detection at the two output modes. Similarly for the Y-basis measurement, two logical encoding can be also discriminated with a modulated beam splitter accordingly.

An essential requirement to guarantee the security of the BB84 protocol is basis indistinguishability, i.e. that Eve cannot distinguish between the logical states encoded in X and Y basis. It can be investigated by the fidelity  $\mathcal{F}_j(\rho_x, \rho_y)$  between the mixed states of the two encoding,  $\rho_x = |0_x\rangle_j\langle 0_x| + |1_x\rangle_j\langle 1_x|$  and  $\rho_y = |0_y\rangle_j\langle 0_y| + |1_y\rangle_j\langle 1_y|$  (the coefficient is omitted). Following the procedure in Ref. [34], its minimum limit can be obtained as

$$\mathcal{F}_j(\rho_x, \rho_y) \geq \frac{d \left| \sum_{q=0}^{d-1} \omega^{jq} e^{-2\mu + \mu\omega^{-q}} (e^{i\mu\omega^{-q}} + i e^{-i\mu\omega^{-q}}) \right|}{\sqrt{2} \mathcal{N}_{2\mu, j}}, \quad (6)$$

details of which is presented in Appendix. The result shows that the encoded logical states in the two bases are more indistinguishable as  $d$  increases or  $\mu$  gets smaller. From the fact that the encoding of X and Y basis are indistinguishable both for Pseudo-single and -vacuum states, we can see that a photon loss in PSP is not significantly detrimental to the security of the QKD.

*Key generation rate-* We analyze the key generation rate of QKD with PSPs. For WCSs, the key generation rate can be estimated based on the Gottesman-Lo-Lütkenhaus-Preskill (GLLP) security analysis as,

$$R \geq -f Q_\mu H(E_\mu) + Q_\mu \Omega \left[ 1 - H(E_\mu/\Omega) \right], \quad (7)$$

where  $Q_\mu$  and  $E_\mu$  are the overall gain and quantum bit error rate (QBER), respectively, for a given mean photon number  $\mu$  of the signal state. Here,  $f$  is the error correction efficiency,  $H(p) = -p \log_2 p - (1-p) \log_2 (1-p)$  is the binary Shannon entropy function, and  $\Omega$  is the fraction of Bob's detection originated from single photon signal emitted from Alice. We take here a pessimistic assumption that all errors are coming from single photon states in the signal. For non-decoy method, the fraction is estimated as  $\Omega = (Q_\mu - P_{\text{multi}})/Q_\mu$ , where  $P_{\text{multi}}$  denotes the probability of Alice's emitting a multi photon state as signal. On the other hand, by using the decoy state method [14–16], the second term in Eq. (7) is replaced with  $Q_1 [1 - H(e_1)]$ , where  $Q_1 = Y_1 \mu e^{-\mu}$  is the gain of the single photon component,  $Y_n$  and  $e_n$  are the yield and QBER for a given photon number  $n$  respectively, and  $\mu e^{-\mu}$  is the probability of generating single photon state in the Poisson distribution. From the underlying assumption of the decoy state method [15], i.e.  $Y_n(\text{decoy}) = Y_n(\text{signal})$  and  $e_n(\text{decoy}) = e_n(\text{signal})$ , Alice can vary  $\mu$  for each signal. The variable  $Y_n$  and  $e_n$  can be deduced with the experimentally measured  $Q_\mu$  and  $E_\mu$ . Therefore, in the decoy state method, Alice can pick up the mean photon number as  $\mu = O(1)$  so that the key rate is obtained as  $O(\eta)$  where  $\eta$  is the overall transmission probability. On the other hand, the optimal  $\mu$  for the non-decoy method is  $\mu = O(\eta)$  yielding the key rate  $R = O(\eta^2)$ . As a result, the decoy method can substantially improve the key generation rate.

Let us estimate the key generation rate with PSPs. Suppose that Alice prepares a setup for generating  $|j_d\rangle$

with probability  $P_j$  in Eq. (3). The transmission probability of a single photon state is  $\eta = 10^{-0.21L/10} \eta_{Bob}$  with the distance  $L$  and the efficiency of transmission and detection on Bob's side  $\eta_{Bob}$ . The transmission probability for  $n$ -photon signals is  $\eta_n = 1 - (1 - \eta)^n$ . The yield is given by  $Y_n = \eta_n + Y_0 - \eta_n Y_0 = 1 - (1 - Y_0)(1 - \eta)^n$  where  $Y_0$  is the dark count rate. The total gain and QBER are obtained then as  $Q_\mu = Y_0 + \sum_{j=0}^{d-1} \sum_{n \in \mathbb{S}_j} \{1 - (1 - \eta)^n\} e^{-\mu} \mu^n / n! = Y_0 + 1 - e^{-\eta\mu}$  and  $Q_\mu E_\mu = e_0 Y_0 + e_{\text{det}}(1 - e^{-\eta\mu})$ , respectively, where  $e_{\text{det}}$  is the detection error rate. For a non-decoy method, the key generation rate of our scheme can be estimated by Eq. (7) with

$$P_{\text{multi}} = \sum_{j=2}^{d-1} P_{\mu, j} = e^{-\mu} \sum_{j=2}^{d-1} \sum_{n \in \mathbb{S}_j} \frac{\mu^n}{n!}. \quad (8)$$

If  $|j_d\rangle$  is identified with a measurement discriminating  $j$  on Alice's side, we can employ decoy state methods:

i) For the case when  $j$  can be fully identified by e.g. heterodyne measurements with the choice of  $\sqrt{\nu} > d$ , it is possible for Alice and Bob to follow the passive decoy state method [35–37]. One additional thing we should take care of is the fact that pseudo-number states have discrete phases so that the encoding with two bases X and Y are not perfectly indistinguishable. The key generation rate is then estimated as

$$R \geq P_1 Y_1 \left[ 1 - f H(e_1^b) - H(e_1^p) \right], \quad (9)$$

with a pessimistic assumption that all errors occur with  $|1_d\rangle$ . Here,  $\Delta_j = (1 - F_j)/2Y_j$  is defined as basis dependence with the fidelity in Eq. (6), and the bit and phase error rates are given respectively by [17]  $e_j^b = (e_0 - e_{\text{det}})(Y_0/Y_j) + e_{\text{det}}$  and  $e_j^p \leq e_j^b + 4\Delta_j(1 - \Delta_j)(1 - 2e_j^b) + 4(1 - 2\Delta_j)\sqrt{\Delta_j(1 - \Delta_j)}e_j^b(1 - e_j^b)$ .

ii) We then consider the case when only PSPs can be discriminated from  $|j(\neq 1)_d\rangle$  e.g. by inefficient on-off detectors as illustrated in Fig. 2(b). The gain and QBER for triggered and non-triggered events are written by

$$\begin{aligned} Q_\mu^{(t)} &= \sum_{j=0}^{d-1} Q_{\mu, \nu, j}^{(t)}, & E_\mu^{(t)} Q_\mu^{(t)} &= \sum_{j=0}^{d-1} Q_{\mu, \nu, j}^{(t)} e_j, \\ Q_\mu^{(nt)} &= \sum_{j=0}^{d-1} Q_{\mu, \nu, j}^{(nt)}, & E_\mu^{(nt)} Q_\mu^{(nt)} &= \sum_{j=0}^{d-1} Q_{\mu, \nu, j}^{(nt)} e_j. \end{aligned} \quad (10)$$

We define the total ratio  $r \equiv Q_\mu^{(t)}/Q_\mu^{(nt)}$  and the ratio for  $j \neq 1$  as  $r_{\nu, j \neq 1} \equiv Q_{\mu, \nu, j}^{(t)}/Q_{\mu, \nu, j}^{(nt)} = \eta_{\nu, j}/\eta_{\nu, j}^{(nt)}$ , which are experimentally known parameters by Eq. (4). From the fact that  $r_{\nu, 2} \geq r_{\nu, j \geq 2}$  and  $r_{\nu, 2} = r_{\nu, 0}$ , we can see that  $Q_{\mu, \nu, j}^{(t)} \leq r_{\nu, 0} Q_{\mu, \nu, j}^{(nt)}$  is always satisfied for  $j \geq 2$ , which can be rewritten by  $Q_\mu^{(t)} - Q_{\mu, \nu, 0}^{(t)} - Q_{\mu, \nu, 1}^{(t)} \leq r_{\nu, 0} (Q_\mu^{(nt)} - Q_{\mu, \nu, 0}^{(nt)})$ . Since its left side is equal to  $r Q_\mu^{(nt)} - r_{\nu, 0} Q_{\mu, \nu, 0}^{(nt)} -$

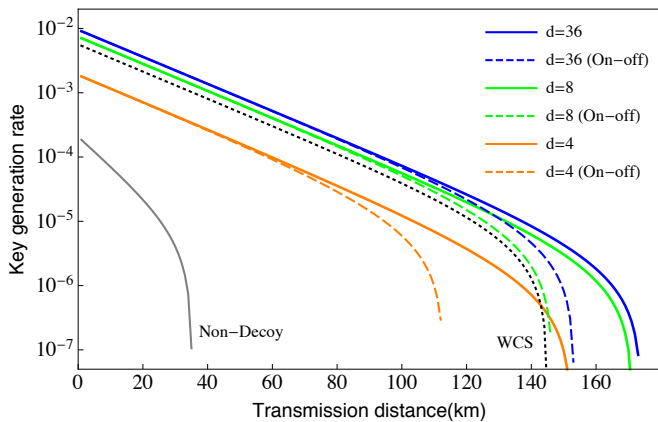


FIG. 4. The key generation rate of the BB84 protocol with PSPs. The solid lines are obtained with a passive decoy state method in the assumption that  $j$  is fully discriminated on Alice side, while the dashed lines are for the case when on-off detectors illustrated in Fig. 2(b) are used. The dotted line is the key rate obtained based on the common approach using phase randomized WCS and an active decoy method. For our simulation, the typical experimental parameters in Ref. [38] are used:  $f = 1.16$ ,  $\eta_{\text{det}} = 0.12$ ,  $\eta_{\text{Bob}} = 0.045$ ,  $Y_0 = 1.7 \times 10^{-6}$  and  $e_{\text{det}} = 0.033$ . The mean photon number in the signal is optimized as  $\mu = 1.0, 0.45, 0.08$  for  $d = 36, 8, 4$ , respectively.

$Q_{\mu,\nu,1}^{(t)}$ , we arrive at  $Q_{\mu,\nu,1}^{(t)} \geq (r - r_{\nu,0})Q_{\mu}^{(nt)}$ . The maximal QBER is also obtained as

$$e_1^b \leq \frac{E_{\mu}^{(t)} Q_{\mu}^{(t)} - e_0 Q_{\mu,\nu,0}^{(t)}}{Q_{\mu,\nu,1}^{(t)}} \quad (11)$$

$$= \frac{r E_{\mu}^{(t)} Q_{\mu}^{(nt)} - e_0 r_{\nu,0} Q_{\mu,\nu,0}^{(nt)}}{Q_{\mu,\nu,1}^{(t)}} \leq \frac{r E_{\mu}^{(t)} Q_{\mu}^{(nt)}}{Q_{\mu,\nu,1}^{(t)}}.$$

As a result, the key generation rate can be estimated by

$$R \geq -f Q_{\mu}^{(t)} H(E_{\mu}^{(t)}) + \min \left\{ Q_{\mu,\nu,1}^{(t)} \left[ 1 - H(e_1^b) \right] \right\}. \quad (12)$$

The key generation rates obtained by our scheme are plotted in Fig. 4. It shows that higher key generation rates can be achieved with PSPs over longer distances than a typical approach using phase randomized WCSs. We note that QKD with PSPs does not require active phase modulation or random number generator that can be possible security loopholes with device imperfections.

*Remarks-* We have introduced pseudo-single photon state (PSP) that mimics a single photon state with respect to both the mean photon number and indeterminate phases. Not only it becomes close to a perfect single photon state with almost unit fidelity but also it exhibits the fundamental behaviors of single photons such as anti-bunching and Hong-Ou-Mandel interference. The emergence and vanishing of single photon characteristics can be observed by changing either the mean photon number  $\mu$  or the number of phase  $d$ . This is contrast to attenuated and/or phase randomized coherent states that never

exhibit such single photon behaviors. It shows the fact that the uncertainty between photon number and phase indeed constitutes the characteristic of single photons.

We also presented a scheme to generate PSPs by employing, but not limited to, atomic vapor in HC-PCF [22, 23, 29–33] that enables cross-phase modulation with fast response time at room temperature. Despite recent progress in cross-phase modulation techniques in various systems [39–45], they were mostly aimed at implementing quantum non-destructive measurements [46] or two-qubit gate operations [47, 48], which are still demanding due to the requirement of either a strong nonlinearity or additional schemes with precise controls [49]. By contrast, a weak nonlinearity even along with source or detector imperfections would suffice to implement our scheme.

We have finally demonstrated that QKD with PSPs achieves higher key generation rates over longer distances than the typical QKD with phase randomized WCSs, as a representative example showing quantum advantage of quantum uncertainty over the statistical randomization. Exploring further applications of PSPs will be the next step of research. We expect that our work opens a way to explore fundamental single photon nature and paves an alternative route to photonic quantum communication.

- 
- [1] W. Wootters and W. Zurek, *Nature* **299** 802-803 (1982).
  - [2] C. H. Bennett and G. Brassard, *Proceedings of IEEE International Conference on Computers, Systems, and Signal Processing*, 175-179 (IEEE Press, 1984).
  - [3] A. K. Ekert, *Phys. Rev. Lett.* **67**, 661 (1991).
  - [4] N. Gisin, G. Ribordy, W. Tittel, and H. Zbinden, *Rev. Mod. Phys.* **74**, 145 (2002).
  - [5] V. Scarani *et al.*, *Rev. Mod. Phys.* **81**, 1301 (2002).
  - [6] H.-K. Lo, M. Curty, and K. Tamaki, *Nature Photonics* **8**, 595 (2014).
  - [7] C. K. Hong, Z. Y. Ou, and L. Mandel, *Phys. Rev. Lett.* **59**, 2044 (1987).
  - [8] Bennett, C. H., Brassard, G., Crepeau, C., Jozsa, R., Peres, A. & Wootters, W. K. Teleporting an unknown quantum state via dual classical and Einstein-Podolsky-Rosen channels. *Phys. Rev. Lett.* **70**, 1895-1899 (1993).
  - [9] Duan, L.-M., Lukin, M. D., Cirac, J. I. & Zoller, P. Long-distance quantum communication with atomic ensembles and linear optics. *Nature* **414**, 413–418 (2001).
  - [10] Pirandola, S., Eisert, J., Weedbrook, C., Furusawa, A. & Braunstein, S. L. Advances in quantum teleportation. *Nature Photonics* **9**, 641–652 (2015).
  - [11] P.-I. Schneider *et al.* *Optics Express* **26**, 8479 (2018).
  - [12] M. D. Eisaman, J. Fan, A. Migdall, and S. V. Polyakov, *Review of Scientific Instruments* **82**, 071101 (2011).
  - [13] I. Aharonovich, D. Englund, and M. Toth, *Nature Photonics* **10**, 631 (2016).
  - [14] W. Y. Hwang, *Phys. Rev. Lett.* **91**, 057901 (2003).
  - [15] H.-K. Lo, X. Ma, and K. Chen, *Phys. Rev. Lett.* **94**, 230504 (2005).
  - [16] X.-B. Wang, *Phys. Rev. Lett.* **94**, 230503 (2005).
  - [17] H.-K. Lo and J. Preskill, *Quantum Inf. Comput.*, **7**, 0431

(2007).

- [18] X. Yuan, Z. Zhang, N. Lütkenhaus, and X. Ma, Phys. Rev. A **94** 062305 (2016)
- [19] P. Valente and A. Lezama, J. Opt. Soc. Am. B **34**, 924 (2017).
- [20] A. Aragoneses, N. T. Islam, M. Eggleston, A. Lezama, J. Kim, and D. J. Gauthier, Optics Letters **43**, 3806-3809 (2018).
- [21] Á. Navarrete, W. Wang, F. Xu, and M. Curty, New J. Phys. **20**, 043018 (2018).
- [22] V. Venkataraman, K. Saha, and A. L. Gaeta, Nature Photonics **7**, 138 (2012).
- [23] C. Perrella, P. S. Light, J. D. Anstie, F. Benabid, T. M. Stace, A. G. White, and A. N. Luiten, Phys. Rev. A **88**, 013819 (2013)
- [24] J. Janszky, P. Domokos, S. Szabo, and P. Adam, Phys. Rev. A **51**, 4191 (1995).
- [25] J. Kim *et al.* Optics Communication **337**, 79 (2015).
- [26] V. V. Dodonov, I. A. Malkin, and V. I. Man'ko, Physica **72**, 597-615 (1974).
- [27] S. J. D. Phoenix, Phys. Rev. A **41**, 5132 (1990).
- [28] H. Paul, Rev. Mod. Phys. **54**, 1061 (1982).
- [29] V. Venkataraman, K. Saha, P. Londero, and A. L. Gaeta, Phys. Rev. Lett **107**, 193902 (2011).
- [30] M. Bajcsy, S. Hofferberth, V. Balic, T. Peyronel, M. Hafezi, A. S. Zibrov, V. Vuletic, and M. D. Lukin, Phys. Rev. Lett **102**, 203902 (2009).
- [31] G. Epple, K.S. Kleinbach, T.G. Euser, N.Y. Joly, T. Pfau, P. St. J. Russell, and R. L'ow, Nature Communications **5**, 4132 (2014).
- [32] M. R. Sprague, P. S. Michelberger, T. F. M. Champion, D. G. England, J. Nunn, X.-M. Jin, W. S. Kolthammer, A. Abdolvand, P. St. J. Russell, and I. A. Walmsley, Nature Photonics **8** 287 (2014).
- [33] C. Perrella, P. S. Light, S. Afshar Vahid, F. Benabid, and A. N. Luiten, Physical Review Applied **9**, 044001 (2018).
- [34] Z. Cao, Z. Zhang, H.-K. Lo, and X. Ma, New J. Phys. **17**, 053014 (2015).
- [35] W. Mauerer and C. Silberhorn, Phys. Rev. A **75**, 050305(R) (2007).
- [36] Y. Adachi, T. Yamamoto, M. Koashi, and N. Imoto, Phys. Rev. Lett. **99**, 180503 (2007).
- [37] X. Ma, and H.-K. Lo, New J. Phys. **10**, 073018 (2008).
- [38] C. Gobby, Z. L. Yuan, and A. J. Shields, Applied Physics Letters **84** 3762 (2004).
- [39] N. Matsuda, R. Shimizu, Y. Mitsumori, H. Kosaka, and K. Edamatsu, Nature Photonics **3**, 95 (2009).
- [40] O. Firstenberg *et al.* Nature **502** 71 (2013).
- [41] I. -C. Hoi *et al.*, Phys. Rev. Lett. **111**, 053601 (2013).
- [42] A. Feizpour, M. Hallaji, G. Dmochowski, and A. M. Steinberg, Nature Physics **11** 905 (2015).
- [43] D. Tiarks, S. Schmidt, G. Rempe, and S. Dürr, Science Advances **2**, e1600036 (2016).
- [44] K. M. Becka, M. Hosseinia, Y. Duana, and V. Vuletić, PNAS **113** 9740 (2016).
- [45] Z. -Y. Liu *et al.*, Phys. Rev. Lett. **117**, 203601 (2016).
- [46] W. J. Munro, K. Nemoto, R. G. Beausoleil, and T. P. Spiller, Phys. Rev. A **71**, 033819 (2005).
- [47] K. Nemoto and W. J. Munro, Phys. Rev. Lett. **93**, 250502 (2004).
- [48] W. J. Munro, K. Nemoto, and T. P. Spiller, New J. Phys. **7**, 137 (2005).
- [49] H. Jeong, Phys. Rev. A **73**, 052320 (2006).

## Appendix

### FIDELITY BETWEEN IDEAL- AND PSEUDO-NUMBER STATES

The pseudo-number states are defined as the maximally superposed states of the coherent states,

$$|j_d\rangle = \frac{1}{\sqrt{\mathcal{N}_{\mu,j}}} \sum_{q=0}^{d-1} \omega^{-jq} |\sqrt{\mu}\omega^q\rangle \quad (\text{A1})$$

$$= \frac{de^{-\mu/2}}{\sqrt{\mathcal{N}_{\mu,j}}} \sum_{n \in \mathbb{S}_j} \frac{\mu^{n/2}}{\sqrt{n!}} |n\rangle, \quad (\text{A2})$$

where  $j \in \{0, 1, \dots, d-1\}$  and the normalization factor is

$$\mathcal{N}_{\mu,j} = d^2 e^{-\mu} \sum_{n \in \mathbb{S}_j} \frac{\mu^n}{\sqrt{n!}}. \quad (\text{A3})$$

For large  $\mu$  (in the regime  $\sqrt{\mu} > d$ ),  $|j_d\rangle$  nearly constitute  $d$ -dimensional orthonormal basis [25]. As  $\mathcal{N}_{\mu,j} \rightarrow d$ ,  $|j_d\rangle$  and  $|\sqrt{\mu}\omega^q\rangle$  are in the discrete Fourier transform relations:  $|\sqrt{\mu}\omega^l\rangle = \hat{F}_d |j_d\rangle$  and  $|k_d\rangle = \hat{F}_d^{-1} |\sqrt{\mu}\omega^j\rangle$ , where  $\hat{F}_d = (1/\sqrt{d}) \sum_{k=0}^{d-1} \sum_{l=0}^{d-1} \omega^{kl} |k_d\rangle \langle l_d|$ . On the other hand, for the small  $\mu$  region,  $|j_d\rangle$  can mimic ideal number states. It becomes closer to  $|j\rangle$  as  $\mu$  gets smaller or  $d$  increases. The fidelity between  $|j_d\rangle$  and  $|j\rangle$  is given by

$$F(|j\rangle, |j_d\rangle) = |\langle j | j_d \rangle|^2 = \left| \frac{d}{\sqrt{\mathcal{N}_{\mu,j}}} e^{-\mu/2} \frac{\mu^{j/2}}{\sqrt{j!}} \right|^2. \quad (\text{A4})$$

The fidelity between ideal and pseudo-single photon (PSP) states

$$F(|1\rangle, |1_d\rangle) = \frac{d^2 e^{-\mu}}{\mathcal{N}_{\mu,1}} = \frac{\mu}{\sum_{n \in \mathbb{S}_1} \mu^n / n!}, \quad (\text{A5})$$

is plotted in Fig. 1(a) in the main text. We can observe that the fidelity approaches to unit as  $\mu$  decreases or  $d$  increases. Note that in the limit  $d \rightarrow \infty$ , we can analytically see  $F(|1\rangle, |1_d\rangle) = \mu/\mu = 1$ , and in the limit  $\mu \rightarrow 0$  with finite  $d$ ,

$$F(|1\rangle, |1_d\rangle) = \frac{\mu}{\mu + \frac{\mu^{d+1}}{(d+1)!} + \frac{\mu^{2d+1}}{(2d+1)!} + \dots} \rightarrow 1. \quad (\text{A6})$$

We thus call  $|1_d\rangle$  with arbitrary small  $\mu$  as pseudo-single photon state (PSP). For the case when  $d = 2$ , PSP becomes so called an odd cat state [26] that is well known to approach  $|1\rangle$  when  $\mu \rightarrow 0$ . Note that, compared to the odd cat states, PSPs with higher  $d$  get closer to single photons in the wider range of  $\mu$ .

## EFFECTS OF PHOTON LOSSES

Let us consider the effect of photon losses on the pseudo-number states in Eq.(1) in the main text. Their evolution in a lossy environment can be evaluated by solving the master equation [27],

$$\frac{d\rho}{dt} = \gamma(\hat{J} + \hat{L})\rho, \quad (\text{A7})$$

where  $\hat{J}\rho = \sum_i \hat{a}_i \rho \hat{a}_i^\dagger$ ,  $\hat{L}\rho = -\sum_i (\hat{a}_i^\dagger \hat{a}_i \rho + \rho \hat{a}_i^\dagger \hat{a}_i)/2$ . Here,  $\hat{a}_i$  ( $\hat{a}_i^\dagger$ ) is the annihilation (creation) operator for the  $i$ -th mode,  $\gamma$  is the decay constant, and  $\eta = e^{-\gamma t}$  is defined as the transmission rate under loss. The pseudo-number state  $|j_d\rangle$  evolves under losses into

$$\rho_j(t) = \frac{1}{\mathcal{N}_{\mu,j}} \sum_{q,q'=0}^{d-1} \omega^{j(q'-q)} e^{(\omega^{q-q'}-1)\mu(1-\eta)} \times |\sqrt{\mu\eta}\omega^q\rangle \langle \sqrt{\mu\eta}\omega^{q'}|. \quad (\text{A8})$$

For PSP with small  $\mu(1-\eta)$ , it can be written by

$$\rho_1(t) = \frac{1}{\mathcal{N}_{\mu,1}} \sum_{q,q'=0}^{d-1} \omega^{q'-q} e^{(\omega^{q-q'}-1)\mu(1-\eta)} \times |\sqrt{\mu\eta}\omega^q\rangle \langle \sqrt{\mu\eta}\omega^{q'}| \approx (1 - \mu(1-\eta)) |1'_d\rangle \langle 1'_d| + \mu(1-\eta) |0'_d\rangle \langle 0'_d| \quad (\text{A9})$$

where  $|1'_d\rangle$  and  $|0'_d\rangle$  are respectively the pseudo-single and -vacuum states with an attenuated amplitude (mean photon number  $\mu\eta$ ).

## SINGLE PHOTON BEHAVIORS

### 1. Antibunching

Antibunching is a single photon characteristics with sub-Poissonian photon statistics, where the 2nd-order correlation function is less than 1,

$$g^{(2)}(0) = \frac{\langle a^\dagger a^\dagger a a \rangle}{\langle a^\dagger a \rangle^2} = \frac{\langle a^\dagger a a^\dagger a \rangle - \langle a^\dagger a \rangle^2}{\langle a^\dagger a \rangle^2} < 1. \quad (\text{A10})$$

Note that coherent states are in Poissonian statistics with  $g^{(2)}(0) = 1$ . The statistics with  $g^{(2)}(0) > 1$  is called super-Poissonian. The 2nd-order correlation function of PSP can be calculated as

$$g^{(2)}(0) = \mathcal{N}_{\mu,1} \frac{\sum_{q,q'=0}^{d-1} \omega^{q'-q} e^{(\omega^{q-q'}-1)\mu}}{(\sum_{q,q'=0}^{d-1} e^{(\omega^{q-q'}-1)\mu})^2}, \quad (\text{A11})$$

for arbitrary given  $\mu$  and  $d$ .

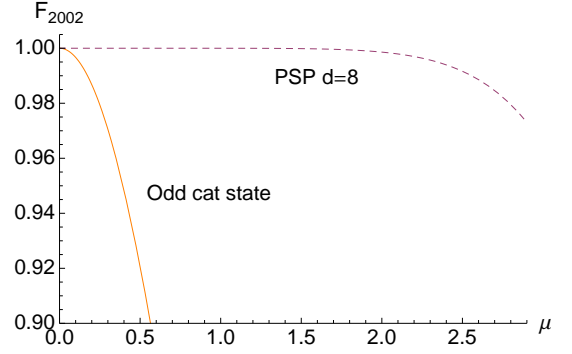


FIG. A1. The fidelity between the state in the output modes of beam splitter and  $|2\rangle|0\rangle - |0\rangle|2\rangle$  (solid) when two odd cat states (PSPs with  $d = 2$ ) enter different input modes, and (dotted) when two PSPs with  $d = 8$  enter.

### 2. Two-photon (Hong-Ou-Mandel) interference

Suppose that two PSPs with arbitrary  $(\mu, d, \delta)$  and  $(\mu', d', \delta')$  respectively, enter different input modes of a 50:50 beam splitter. The state in the two output mode can be then written as

$$|1_d\rangle|1'_d\rangle \xrightarrow{BS} |out\rangle = \frac{1}{\sqrt{\mathcal{N}_{\mu,1}\mathcal{N}_{\mu',1}}} \sum_{q=0}^{d-1} \sum_{q'=0}^{d-1} \omega_d^{-q-\delta} \omega_{d'}^{-q'-\delta'} \times \left| \frac{\sqrt{\mu}\omega_d^{q+\delta} + \sqrt{\mu'}\omega_{d'}^{q'+\delta'}}{\sqrt{2}} \right\rangle \left| \frac{\sqrt{\mu}\omega_d^{q+\delta} - \sqrt{\mu'}\omega_{d'}^{q'+\delta'}}{\sqrt{2}} \right\rangle, \quad (\text{A12})$$

where we use subscript in  $\omega_d = \exp(2\pi i/d)$  to distinguish different  $d$ . We can calculate the probability for detecting photons in both out modes (with on-off photon detectors) by

$$P_{11}(\mu, d, \delta|\mu', d', \delta') = \langle out | (\mathbb{1} - |0\rangle\langle 0|) \otimes (\mathbb{1} - |0\rangle\langle 0|) |out\rangle,$$

and also the fidelity between the state in output modes and  $(|2\rangle|0\rangle - |0\rangle|2\rangle)/\sqrt{2}$  as

$$F_{2002}(\mu, d, \delta|\mu', d', \delta') = |\langle out | (|2\rangle|0\rangle - |0\rangle|2\rangle) / \sqrt{2} \rangle|^2.$$

We first analyze the case when two identical PSPs enter the input modes, i.e.  $\mu = \mu'$ ,  $d = d'$ , and  $\delta = \delta'$  as presented in the main text. Two-photon interference is clearly observed with such PSPs, which tends to be clearer as  $\mu$  decreases and  $d$  increases. We note that although  $P_{11}$  of an odd cat state (PSP with  $d = 2$ ) is always zero for any  $\mu$ , its  $F_{2002}$  is only close to 1 when  $\mu \rightarrow 0$  as plotted in Fig A1. Thus, two odd cat states with nonzero  $\mu$  do not exhibit two-photon interference, while PSPs with higher  $d$  can exhibit it in a wider range of  $\mu$ . For example, PSPs with  $d = 8$  and  $\mu \lesssim 2$  show perfect two-photon interference ( $P_{11} = 0$  and  $F_{2002} = 1$ ) as shown in Fig. A1.

We plot  $P_{11}(\mu, d, \delta|\mu', d', \delta')$  and  $F_{2002}(\mu, d, \delta|\mu', d', \delta')$  in Fig. A2 with exemplary parameters, which evidently

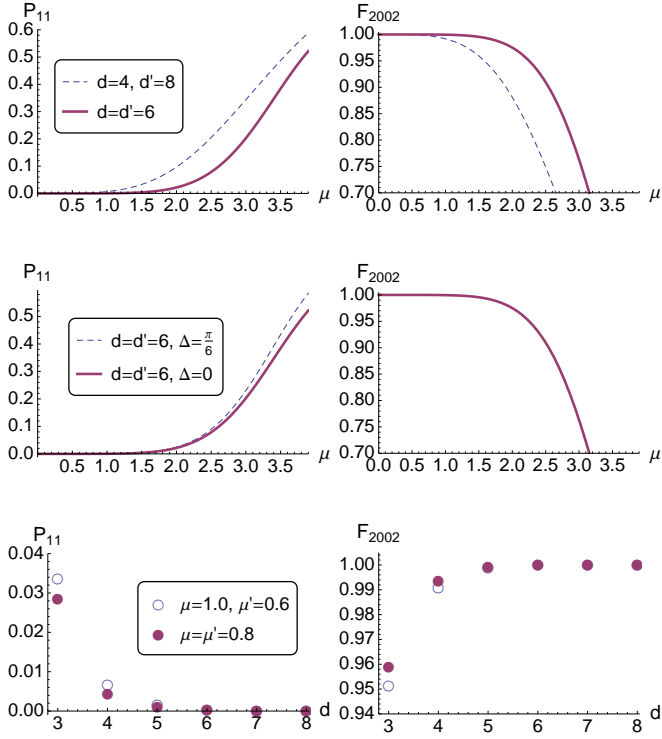


FIG. A2. Comparisons of  $P_{11}$  and  $F_{2002}$  between the case when the same PSPs enter the input modes and the case when two different PSPs enter (different  $d$  for upper two plots, different  $\delta$  for middle two, and different  $\mu$  for lower two). Here,  $\Delta \equiv (2\pi/d)(\delta - \delta')$  denotes the difference of reference phases of two input PSPs.

show two-photon interference between two different PSPs with either  $\mu \neq \mu'$ ,  $\delta \neq \delta'$ , or  $d \neq d'$ . We note that, among all the pair of PSPs with fixed  $\mu + \mu'$  and  $d + d'$ , two PSPs with  $\mu = \mu'$ ,  $d = d'$  and  $\delta = \delta'$  exhibit the strongest interference as one can see from the results in Fig. A2. This can be understood as the fact that they are the most indistinguishable among all possible pairs of PSPs.

## GENERATION SCHEME

### Cross phase modulation with atomic vapor in hollow-core photonic crystal fiber

We first consider a feasible scheme of cross phase modulation, aiming to apply for generating PSPs: Atomic vapor filled in hollow-core photonic crystal fiber (HC-PCF) is an efficient platform for photon-level quantum processors [22, 23, 29–33] such as cross phase modulation [22, 23], all-optical switches [29, 30], and quantum memories [32]. Particularly, cross phase modulation has been realized with rubidium (Rb) atoms con-

fining in HC-PCF [22, 23]. The energy level of  $^{85}\text{Rb}$  illustrated in Fig. A3 is the basis of the nonlinear interaction. A weak laser (780.2 nm) in mode 1 tuned closely to the  $5S_{1/2} \rightarrow 5P_{3/2}$  transition induces a phase shift on a stronger laser (776 nm) in mode 2 tuned closely to the  $5P_{3/2} \rightarrow 5D_{5/2}$  transition. This nonlinear interaction can be characterized with the 3rd-order susceptibility  $\chi^{(3)} \approx (N\mathfrak{d}_1\mathfrak{d}_2)/(\epsilon_0\hbar^3\Delta_1^2\Delta_2)$ , where  $N$  is the atomic number density,  $\mathfrak{d}_1$  and  $\mathfrak{d}_2$  are the transition dipole moments for  $5S_{1/2} \rightarrow 5P_{3/2}$  and  $5P_{3/2} \rightarrow 5D_{5/2}$ , respectively. The induced phase shift in mode 1 can be given by  $\phi_1 \sim (k_1 n_2 P_2 L)/A$  with optimal detuning  $\Delta_1 \approx \Delta_2$ , where  $k_1$  is the wavenumber in mode 1,  $n_2$  is the nonlinear refractive index,  $P_2$  is the power of the beam in mode 2,  $L$  is the length of the vapor-filled fiber, and  $A$  is the optical mode area. Exemplary schemes with detailed descriptions are in Ref. [22, 23], which achieved the cross phase shift up to 0.3 mrad per photon with fast response time ( $< 5$  ns) and low absorption ( $< 1\%$ ) at room temperature [22]. Moreover, cross phase shift up to  $\pi$  has been also demonstrated (e.g. with  $P_2 \approx 25\mu\text{W}$ ), as  $\phi_1$  is proportional to  $P_2$  (in the case without atomic saturation) [23]. Note that the shifted phase is guaranteed not to be induced from self-Kerr effects within this approach [22, 23]. Further improvements are expected by reducing the core diameter, increasing the atomic density, and extending  $L$ .

## Generating PSPs

Assume that lasers in coherent states  $|\sqrt{\mu}\rangle_1|\sqrt{\nu}\rangle_2$  go through the two modes (1 for signal 2 for meter) of atomic vapor filled HC-PCF as illustrated in Fig. A3 and experience the interaction Hamiltonian  $-\hbar\chi^{(3)}\hat{n}_1\hat{n}_2$  for time  $t$ . We also assume that  $\mu$  is small, while  $\nu$  is large enough such that  $\sqrt{\nu} > 2\pi/\chi^{(3)}t$ , and, without loss of the generality, set  $d \equiv 2\pi/\chi^{(3)}t$  as an integer  $\geq 2$ . Then, the

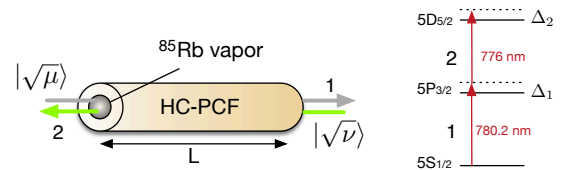


FIG. A3. Cross phase modulation with  $^{85}\text{Rb}$  vapor filled HC-PCF can be used as a platform for generating PSPs. Right:  $^{85}\text{Rb}$  energy level.



output states can be obtained by

$$\begin{aligned}
& e^{\frac{2\pi i}{d}\hat{n}_1\hat{n}_2}|\sqrt{\mu}\rangle_1|\sqrt{\nu}\rangle_2 \\
&= e^{\frac{2\pi i}{d}\hat{n}_1\hat{n}_2}\left(\frac{1}{\sqrt{d}}\sum_{j=0}^{d-1}\sqrt{\frac{\mathcal{N}_{\mu,j}}{d}}|j_d\rangle\right)_1\left(\frac{1}{\sqrt{d}}\sum_{k=0}^{d-1}|k_d\rangle\right)_2 \\
&= \frac{1}{\sqrt{d}}\sum_{j=0}^{d-1}\sqrt{\frac{\mathcal{N}_{\mu,j}}{d}}|j_d\rangle_1\left(\frac{1}{\sqrt{d}}\sum_{k=0}^{d-1}\omega^{jk}|k_d\rangle\right)_2 \\
&= \sum_{j=0}^{d-1}\frac{\sqrt{\mathcal{N}_{\mu,j}}}{d}|j_d\rangle_1|\sqrt{\nu}\omega^j\rangle_2.
\end{aligned}$$

### MINIMUM FIDELITY FOR BASIS INDEPENDENCE

Let us calculate the fidelity between the mixed states of the X and Y basis encoding (the coefficient is omitted),  $\rho_x = |0_x\rangle_j\langle 0_x| + |1_x\rangle_j\langle 1_x|$  and  $\rho_y = |0_y\rangle_j\langle 0_y| + |1_y\rangle_j\langle 1_y|$ , to investigate the basis independence:

$$\begin{aligned}
\mathcal{F}_j(\rho_x, \rho_y) &= \mathcal{F}_j\left(|0_x\rangle_j\langle 0_x| + |1_x\rangle_j\langle 1_x|, |0_y\rangle_j\langle 0_y| + |1_y\rangle_j\langle 1_y|\right) \\
&\geq \mathcal{F}_j\left[|-\rangle|0_x\rangle + |+\rangle|1_x\rangle, |+\rangle|0_y\rangle + |-\rangle|1_y\rangle\right],
\end{aligned}$$

which is derived from the fact that the fidelity of two mixed states is the maximum of their purification [34]. By some calculations, we arrive at the minimum fidelity for basis independence,

$$\mathcal{F}_j(\rho_x, \rho_y) \geq \frac{d\left|\sum_{q=0}^{d-1}\omega^{jq}e^{-2\mu+\mu\omega^{-q}}(e^{i\mu\omega^{-q}} + ie^{-i\mu\omega^{-q}})\right|}{\sqrt{2}\mathcal{N}_{2\mu,j}}.$$

We plot the basis independence,  $\mathcal{F}_j$ , for  $|0_d\rangle$  and  $|1_d\rangle$  in Fig. A4 by changing  $\mu$  with different  $d$ . It shows that the encoded logical states in the two (X and Y) bases are more indistinguishable as  $d$  increases or  $\mu$  decreases.

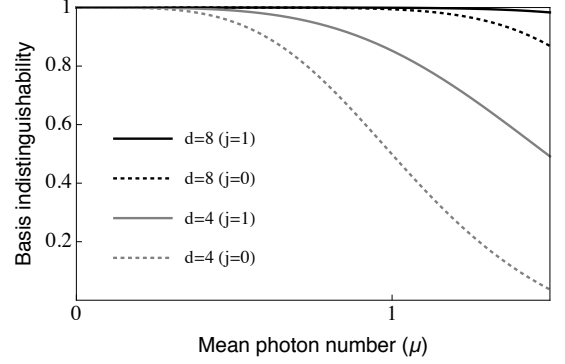


FIG. A4. The basis indistinguishabilities (between X and Y basis) are plotted by changing  $\mu$  for  $d = 4, 8$ . The solid lines denote the basis indistinguishabilities for  $|1_d\rangle$ , while the dotted lines for  $|0_d\rangle$ .

Since the encoding of X and Y basis are indistinguishable both in  $|0_d\rangle$  and  $|1_d\rangle$ , a photon loss in PSP is not significantly detrimental to the security of QKD.